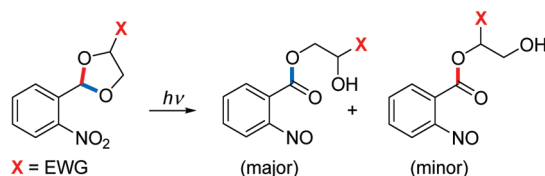


## Photochemistry of 2-Nitrobenzylidene Acetals<sup>†</sup>

Peter Šebej, Tomáš Šolomek, Lubica Hroudná, Pavla Brancová, and Petr Klán\*  
Department of Chemistry, Faculty of Science, Masaryk University, Kamenice 5/A8, 625 00 Brno,  
Czech Republic

klan@sci.muni.cz

Received August 13, 2009



Photolysis of dihydroxy compounds (diols) protected as 2-nitrobenzylidene acetals (ONBA) and subsequent acid- or base-catalyzed hydrolysis of the 2-nitrosobenzoic acid ester intermediates result in an efficient and high-yielding release of the substrates. We investigated the scope and limitations of ONBA photochemistry and expanded upon earlier described two-step procedures to show that the protected diols of many structural varieties can also be liberated in a one-pot procedure. In view of the fact that the acetals of nonsymmetrically substituted diols are converted into one of the corresponding 2-nitrosobenzoic acid ester isomers with moderate to high regioselectivity, the mechanism of their formation was studied using various experimental techniques. The experimental data were found to be in agreement with DFT-based quantum chemical calculations that showed the preferential cleavage occurs on the acetal C–O bond in the vicinity of more electron-withdrawing (or less electron-donating) groups. The study also revealed considerable complexity in the cleavage mechanism and that the structural variations in the substrate can significantly alter the reaction pathway. This deprotection strategy was found to be also applicable for 2-thioethanol when released from the corresponding monothioacetal in the presence of a reducing agent, such as ascorbic acid.

### Introduction

Intramolecular photoreduction of the nitro group and subsequent liberation of a leaving group (LG) from the benzylic position of the 2-nitrobenzyl (*o*-nitrobenzyl; ONB) chromophore belong among the most intensively studied transformations in photochemistry.<sup>1–5</sup> Since its first use as a photo-removable protecting group (PPG),<sup>6</sup> the ONB moiety has been

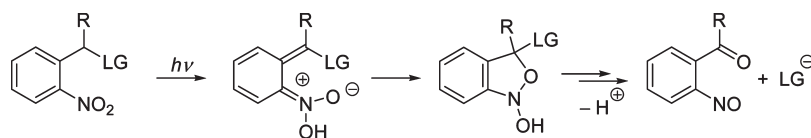
employed in biochemistry,<sup>7,8</sup> organic synthesis,<sup>9</sup> and related fields. Various authors investigated the mechanism of the leaving group release.<sup>10–18</sup> In general, the reaction is initiated by a light-induced intramolecular 1,5-hydrogen shift in the primary step yielding *aci*-nitro intermediates, followed by formation of benzoxazolines and subsequent ring opening to give LG and 2-nitrosoacetophenone as a side product (Scheme 1).

<sup>†</sup> Dedicated to the memory of Professor Peter J. Wagner.

(1) Pelliccioli, A. P.; Wirz, J. *Photochem. Photobiol. Sci.* **2002**, *1*, 441.  
(2) Goeldner, M.; Givens, R. S. *Dynamic Studies in Biology*; Wiley-WCH: Weinheim, 2005.  
(3) Bochet, C. G. *J. Chem. Soc., Perkin Trans. 1* **2002**, 125.  
(4) Givens, R. S.; Conrad, P. G.; Yousef, A. L.; Lee, J.-I. In *CRC Handbook of Organic Photochemistry and Photobiology*; Horspool, W. M., Lenci, F., Eds.; CRC Press: Boca Raton, 2004; p 1.  
(5) Morrison, H. *Biological Applications of Photochemical Switches*; John Wiley and Sons, Inc.: New York, 1993; Vol. 2.  
(6) Kaplan, J. H.; Forbush, B.; Hoffman, J. F. *Biochemistry* **1978**, *17*, 1929.  
(7) Mayer, G.; Heckel, A. *Angew. Chem., Int. Ed.* **2006**, *45*, 4900.  
(8) Ellis-Davies, G. C. R. *Nat. Methods* **2007**, *4*, 619.  
(9) Guillier, F.; Orain, D.; Bradley, M. *Chem. Rev.* **2000**, *100*, 2091.

(10) Zhu, Q. Q.; Schnabel, W.; Schupp, H. *J. Photochem.* **1987**, *39*, 317.  
(11) Corrie, J. E. T.; Barth, A.; Munasinghe, V. R. N.; Trentham, D. R.; Hutter, M. C. *J. Am. Chem. Soc.* **2003**, *125*, 8546.  
(12) Dunkin, I. R.; Gebicki, J.; Kiszka, M.; Sanin-Leira, D. *Spectrochim. Acta, Part A* **1997**, *53*, 2553.  
(13) Schwörer, M.; Wirz, J. *Helv. Chim. Acta* **2001**, *84*, 1441.  
(14) Gaplovsky, M.; Il'ichev, Y. V.; Kamdzhilov, Y.; Kombarova, S. V.; Mac, M.; Schwörer, M. A.; Wirz, J. *Photochem. Photobiol. Sci.* **2005**, *4*, 33.  
(15) Il'ichev, Y. V.; Schwörer, M. A.; Wirz, J. *J. Am. Chem. Soc.* **2004**, *126*, 4581.  
(16) Laimgruber, S.; Schmierer, T.; Gilch, P.; Kiewisch, K.; Neugebauer, J. *Phys. Chem. Chem. Phys.* **2008**, *10*, 3872.  
(17) Bley, F.; Schaper, K.; Görner, H. *Photochem. Photobiol.* **2008**, *84*, 162.  
(18) Hellrung, B.; Kamdzhilov, Y.; Schwörer, M.; Wirz, J. *J. Am. Chem. Soc.* **2005**, *127*, 8934.

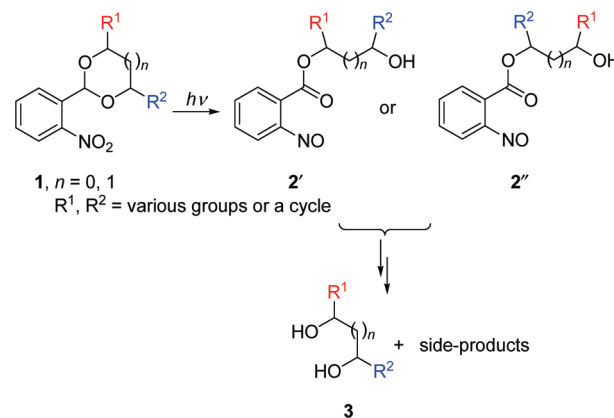
SCHEME 1



The ONB moiety has been used to protect the hydroxy group, for example, in some oligo- and polysaccharides,<sup>19–23</sup> whereas 2-nitrobenzylidene acetals (ONBA, **1**; Scheme 2) can be utilized for protection of dihydroxy compounds (diols). The earlier works of Tanasescu and co-workers (e.g., refs 24 and 25) suggested that 2-nitrosobenzoic acid esters (**2'** and **2''** in Scheme 2) are obtained as primary isolable products after photolysis of **1** and that the corresponding free diols **3** can be liberated by subsequent acid hydrolysis. Collins and co-workers later investigated the photochemistry of various glycosides and pyranosides, in which either the 1,2- or 1,3-dihydroxy functionality was protected as an ONBA.<sup>22,26,27</sup> The 2-nitrobenzylidene acetals of such nonsymmetrically substituted dihydroxy compounds were reported to form preferentially one of two possible 2-nitrosobenzoic acid esters upon photolysis. Young and Deiters have recently used this strategy to control activation of gene expression in bacterial cells.<sup>28</sup> In this case, photolysis of a galactoside acetal gave an ester that was converted to the corresponding dihydroxy compound by intracellular hydrolysis. An inverted procedure of diol release, according to which methylglucoside or methylmannoside ONBA derivatives were treated by boron trifluoride in the first step to release a protected ONB ether followed by photochemical release of the corresponding carbohydrates, was introduced by Iwamura and co-workers.<sup>29</sup> Photorelease of organic diols has also been accomplished using different PPGs, such as salicylaldehyde<sup>30</sup> or coumarin-4-ylmethyl<sup>31</sup> derivatives. In a reverse fashion, carbonyl compounds can be liberated from 2-nitrophenylethylene glycol<sup>32</sup> or bis(2-nitrophenyl)ethanediol<sup>33</sup> precursors.

Here we present a study that was aimed to find the scope and limitations of 2-nitrobenzylidene acetal utilization as a photoremovable group for 1,2- and 1,3-dihydroxy compounds as well as for 2-hydroxythiols. A series of experiments and DFT-based quantum chemical calculations were performed to determine the key steps of the reaction and to understand effects that lead to the remarkable regioselective acetal C–O bond cleavages reported by Collins and

SCHEME 2



co-workers<sup>22,26,27</sup> three decades ago. Furthermore, a simple, one-pot photoinitiated procedure enabling diol release from ONBA in high chemical yields is introduced.

## Results and Discussion

**Preparative Deprotection of Dihydroxy Compounds.** The 2-nitrobenzylidene acetals **1a–f** and the monothioacetal **4** (Table 1) were prepared from the corresponding dihydroxy compounds **3a–f** and 2-thioethanol (**5**), respectively, using 2-nitrobenzaldehyde and *p*-toluenesulfonic acid (PTSA) as a catalyst under azeotropic reflux conditions in a Dean–Stark apparatus (Scheme 3).<sup>34,35</sup> The compounds were obtained in very good chemical yields (88–95%) and purity. The 2-nitrobenzylidene acetal of methyl- $\alpha$ -D-glucopyranoside **1g** was prepared from the corresponding glucopyranoside **3g** and 2-nitrobenzaldehyde by stirring in dioxane with H<sub>2</sub>SO<sub>4</sub> as a catalyst at 20 °C.<sup>36,37</sup>

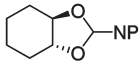
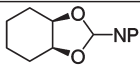
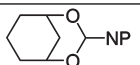
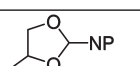
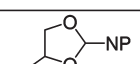
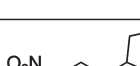


Diol liberation from the acetal **1** proceeds through two key steps: the 2-nitrosobenzoic acid ester intermediate **2** is formed upon acetal irradiation, and the corresponding diol **3** is obtained in a subsequent hydrolysis of **2** (Scheme 2). For this work, two different strategies of diol release have been used.

In *stepwise* procedures, a benzene solution of an acetal (**1a–g**;  $\sim 5 \times 10^{-3}$  M) was irradiated at  $>280$  nm (Pyrex filter) to a nearly complete conversion ( $>95\%$ ). It was apparent that formation of strongly absorbing nitroso intermediates slowed down the observed rate of conversion as their concentration increased as the result of an optical filter effect. The solvent was then evaporated, the remaining material was dissolved in methanol containing NaOH (0.2 M), and the mixture was stirred at 20 °C for approximately 1 h. A liberated diol was isolated by methanol evaporation and subsequent extraction into ethyl acetate after addition of

- (19) Corrie, J. E. T. *J. Chem. Soc., Perkin Trans. 1* **1993**, 2161.  
 (20) Zehavi, U. *Adv. Carbohydr. Chem. Biochem.* **1988**, *46*, 179.  
 (21) Zehavi, U.; Patchornik, A. *J. Org. Chem.* **1972**, *37*, 2285.  
 (22) Collins, P. M.; Oparaech, N. N. *J. Chem. Soc., Perkin Trans. 1* **1975**, 1695.  
 (23) Collins, P. M.; Oparaech, N. N.; Munasinghe, V. R. N. *J. Chem. Soc., Perkin Trans. 1* **1975**, 1700.  
 (24) Tanasescu, I.; Ionescu, M. *Bull. Soc. Chim. Fr.* **1940**, *7*, 77.  
 (25) Tanasescu, I.; Ionescu, M. *Bull. Soc. Chim. Fr.* **1940**, *7*, 84.  
 (26) Collins, P. M.; Munasinghe, V. R. N. *J. Chem. Soc., Perkin Trans. 1* **1983**, 1879.  
 (27) Collins, P. M.; Munasinghe, V. R. N. *J. Chem. Soc., Perkin Trans. 1* **1983**, 921.  
 (28) Young, D. D.; Deiters, A. *Angew. Chem., Int. Ed.* **2007**, *46*, 4290.  
 (29) Watanabe, S.; Sueyoshi, T.; Ichihara, M.; Uehara, C.; Iwamura, M. *Org. Lett.* **2001**, *3*, 255.  
 (30) Kostikov, A. P.; Popik, V. V. *Org. Lett.* **2008**, *10*, 5277.  
 (31) Lin, W. Y.; Lawrence, D. S. *J. Org. Chem.* **2002**, *67*, 2723.  
 (32) Gravel, D.; Hebert, J.; Thoraval, D. *Can. J. Chem.* **1983**, *61*, 400.  
 (33) Blanc, A.; Bochet, C. G. *J. Org. Chem.* **2003**, *68*, 1138.

- (34) Cole, E. R.; Crank, G.; Minh, H. T. H. *Aust. J. Chem.* **1980**, *33*, 675.  
 (35) Jin, T. S.; Zhang, S. L.; Wang, X. F.; Guo, J. J.; Li, T. S. *J. Chem. Res., Synop.* **2001**, 289.  
 (36) Collins, P. M.; Oparaech, N. N. *Carbohydr. Res.* **1974**, *33*, 35.  
 (37) Collins, P. M.; Oparaech, N. N.; Whitton, B. R. *J. Chem. Soc., Chem. Commun.* **1974**, 292.

TABLE 1. Synthesis and Photolysis of Acetals 1a–g and Monothioacetal 4

compound <sup>a</sup>	synthesis <sup>b</sup>	photorelease of 3a–f or 5 <sup>d</sup>	
	(yields / %)	“stepwise” protocol (yields / %)	“one-pot” protocol (yields / %)
 (1a)	93	90 [77 <sup>e</sup> ]	90 [77 <sup>e</sup> ]
 (1b)	95	90 [65 <sup>e</sup> ]	n.c. <sup>g</sup>
 (1c)	95 <sup>c</sup>	81 [67 <sup>e</sup> ]	92 [85 <sup>e</sup> ]
 (1d)	88	85 <sup>d</sup> [75 <sup>e</sup> ]	95 <sup>f</sup>
 (1e)	95	90 <sup>e</sup>	90 <sup>e</sup>
 (1f)	94	86 <sup>f</sup>	96 <sup>f</sup>
 (1g)	36	82 <sup>f</sup>	95 <sup>f</sup>
 (4)	95	90 <sup>f, h</sup>	90 <sup>i, f</sup>

<sup>a</sup>NP = 2-nitrophenyl. <sup>b</sup>Isolated yields; an average of two experiments; two diastereomers were identified by NMR or/and GC in approximately 1:1 ratio in some cases. <sup>c</sup>A mixture of *cis* and *trans* isomers obtained from the commercially available starting material. <sup>d</sup>Photolysis of 1a–g or 4 at > 280 nm in benzene (2-step procedure) or in methanolic NaOH solution (“one-pot” arrangement). Isolated chemical yields obtained using a triple extraction. <sup>e</sup>Isolated yields obtained from a single extraction. <sup>f</sup>Determined by NMR. <sup>g</sup>n.c. = not carried out. <sup>h</sup>Bis(2-hydroxyethyl) disulfide (6) was the exclusive product formed. 2-Thioethanol (5) was obtained in 90% yield only when ascorbic acid (> 4 equiv) as a reducing agent was present during the photolysis; see the text. <sup>i</sup>Irradiated in the presence of ascorbic acid (> 4 equiv).

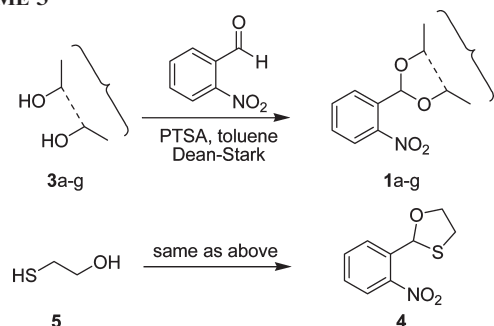
water. The aliphatic diols 3a–d are partially soluble in water; therefore, at least a triple extraction protocol was necessary to attain high chemical yields (Table 1). The sufficiently lipophilic diol 3e was obtained in high yield by using a single extraction. The quantum yields of 1a–e disappearance in various solvents are listed in Table 2. Photodegradation of simple 2-nitrobenzyl esters is known to be rather inefficient ( $\Phi$  is usually below 0.1).<sup>17,38</sup> Yip and co-workers reported

that 2-nitrobenzaldehyde acetal of 2,2-dimethylpropane-1,3-diol photoreacts more efficiently than 2-nitrobenzyl acetate by a factor of 23.<sup>38</sup> The larger disappearance quantum yields of ONBA derivatives reported in Table 2 are in agreement with this observation.

A more convenient *one-pot* procedure, in which the acetals 1 ( $\sim 5 \times 10^{-3}$  M) were photolyzed in 0.2 M NaOH methanolic solutions at 20 °C, directly afforded the corresponding dihydroxy compounds 3. The course of the reaction was followed by NMR to find optimum experimental conditions. The reaction mixture was processed similarly to the second step of the

(38) Yip, R. W.; Sharma, D. K.; Giasson, R.; Gravel, D. *J. Phys. Chem.* 1985, 89, 5328.

SCHEME 3

TABLE 2. Disappearance Quantum Yields for 1a–e ( $\Phi_{\text{dis}}$ ) in Various Solvents at 313 nm

compound	solvent	$\Phi_{\text{dis}}^a$
1a	methanol	$0.38 \pm 0.04$
	hexane	$0.39 \pm 0.05$
1b	methanol	$0.38 \pm 0.08$
	hexane	$0.31 \pm 0.03$
1c	methanol	$0.30 \pm 0.08$
1e	methanol	$0.44 \pm 0.07$

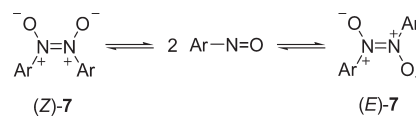
<sup>a</sup>The quantum yields were obtained using 2-nitrobenzaldehyde (for 1a–c;  $\Phi = 0.38$  in methanol<sup>39</sup>) or valerophenone (for 1e,  $\Phi$  of acetophenone formation = 0.33 in hexane<sup>40</sup>) as actinometers. The results are based on at least three independent measurements; the relative standard deviations are shown.

procedure described above. The chemical yields were comparable or better than those of the stepwise procedure (Table 1) despite the fact that photolysis time to obtain sufficiently large conversion (>95%) was somewhat longer (>2 h).

**Chemical Properties of 2-Nitrosobenzoic Acid Ester Intermediates.** To study properties and hydrolytic reaction of 2-nitrosobenzoic acid ester intermediates (**2**), a pentane solution of **1** ( $5 \times 10^{-3}$  M) was irradiated at >280 nm to form **2** as a precipitate. For example, photolysis of **1a** gave the 2-nitrosobenzoic acid ester intermediate in ~60% chemical yield. Aromatic nitroso compounds are known to exist in equilibrium with the corresponding azodioxy dimers ((*E*)- and (*Z*)-**7**; Scheme 4) in solutions.<sup>41,42</sup> The monomer and dimer species can be distinguished by NMR thanks to the shielding anisotropy of the NO group.<sup>43,44</sup> The population of dimers are pronounced at lower temperatures and in the solid state. Since nonsymmetrically substituted acetals, such as **1d–g**, give two different 2-nitrosobenzoic acid esters (Scheme 2), a complex mixture of species was always observed after extensive photolysis.

<sup>1</sup>H NMR analysis of the monomer/dimer equilibrium of **2d** ( $\sim 3 \times 10^{-2}$  M) in CD<sub>3</sub>OD revealed that the concentration of monomers is very small at  $-7$  °C, whereas their population increases considerably at  $+55$  °C (Figure 1). This process was fully reversible over three cooling/heating cycles. The isomer identification was accomplished by comparing the characteristic peaks of the aromatic proton in the *ortho*

SCHEME 4



position to the nitroso group at  $+55$  °C in **2d** (monomer) to that in **2d** (dimer) at  $-7$  °C (Figure 1).

**Photolysis of Nonsymmetric 2-Nitrosobenzylidene Acetals.** More than 30 years ago, Collins and Oparaeché reported that photolysis of ONBA derivatives of some glycosides or pyranosides, which gave the corresponding ONB esters, can be highly regioselective. Two examples are shown in Scheme 5.<sup>22,23</sup> The regioisomers were identified by <sup>1</sup>H NMR measurements either directly or after oxidation of the products to the corresponding 2-nitrobenzoates by trifluoroperacetic acid. These rather unexpected results were attributed to steric and stereoelectronic effects.

One of the goals of our study was to determine the key steps of the reaction and distinguish effects that lead to regioselective acetal C–O bond cleavage in nonsymmetric ONBA derivatives. The structures of regioisomeric 2-nitrosobenzoic acid esters photoreleased from the model ONBA derivatives **1d–g** were analyzed by 2D NMR. The <sup>1</sup>H NMR spectra differentiated the aliphatic hydrogens of the ester group in order to calculate the relative concentrations of the major and minor isomers, while the <sup>1</sup>H–<sup>1</sup>H COSY measurements (see Supporting Information) established the relationships among the neighboring hydrogens in the aliphatic part of the molecule. In addition, <sup>1</sup>H–<sup>13</sup>C HMBC experiments (see Supporting Information) provided an unambiguous correlation between the aliphatic and aromatic parts of the molecule to assign the correct structures. To work with less complex spectra, the samples were analyzed at  $+55$  °C to ensure that the concentration of the azodioxy dimers (Scheme 4) was negligible. The relative concentrations of the regioisomers **2d–g** obtained by irradiation of **1d–g** are given in Scheme 6. The diol substitution indeed affected the regioselective cleavage of the acetal C–O bonds: photolysis of **1d** (R = methyl) gave **2d<sub>a</sub>** as the major product, while an opposite regioisomer **2f<sub>b</sub>** was formed from **1f** (R = 3-nitrophenyl). The phenyl substitution in **1e** had no apparent effect on the reaction regioselectivity. The photoproduct concentration ratio was not affected much by either changing the solvent polarity or by addition of a strong acid. To authenticate our results with those of Collins and Oparaeché,<sup>22,23</sup> **1g** was irradiated in methanol to release a 2.9-fold excess of the glucopyranoside derivative **2g<sub>a</sub>**. This was a very similar observation to that found for the trimethoxy analogue **9**<sup>22,23</sup> (Scheme 5).

We have also investigated the possibility that attack of a nucleophile, such as methanol or water, can participate in an acetal ring opening. No methanol adducts were identified in the reaction mixtures after ONBA derivatives were photolyzed in methanol. In addition, solutions of **1d** in benzene-*d*<sub>6</sub> or methanol-*d*<sub>4</sub>, containing either a small amount of D<sub>2</sub><sup>16</sup>O or isotopically labeled D<sub>2</sub><sup>18</sup>O, were extensively irradiated and the major reaction products were analyzed by LC-MS TOF. The same mass spectra of the photoproducts were obtained in both cases; that is, no incorporation of oxygen from water occurred either during the initial photoreaction or the subsequent dark steps.

(39) George, M. V.; Scaiano, J. C. *J. Phys. Chem.* **1980**, *84*, 492.

(40) Wagner, P. J.; Kemppainen, A. E.; Kochevar, I. E. *J. Am. Chem. Soc.* **1972**, *94*, 7489.

(41) Azoulay, M.; Wettermark, G. *Tetrahedron* **1978**, *34*, 2591.

(42) Azoulay, M.; Stymne, B.; Wettermark, G. *Tetrahedron* **1976**, *32*, 2961.

(43) Fletcher, D. A.; Gowenlock, B. G.; Orrell, K. G. *J. Chem. Soc., Perkin Trans. 2* **1998**, 797.

(44) Fletcher, D. A.; Gowenlock, B. G.; Orrell, K. G. *J. Chem. Soc., Perkin Trans. 2* **1997**, 2201.

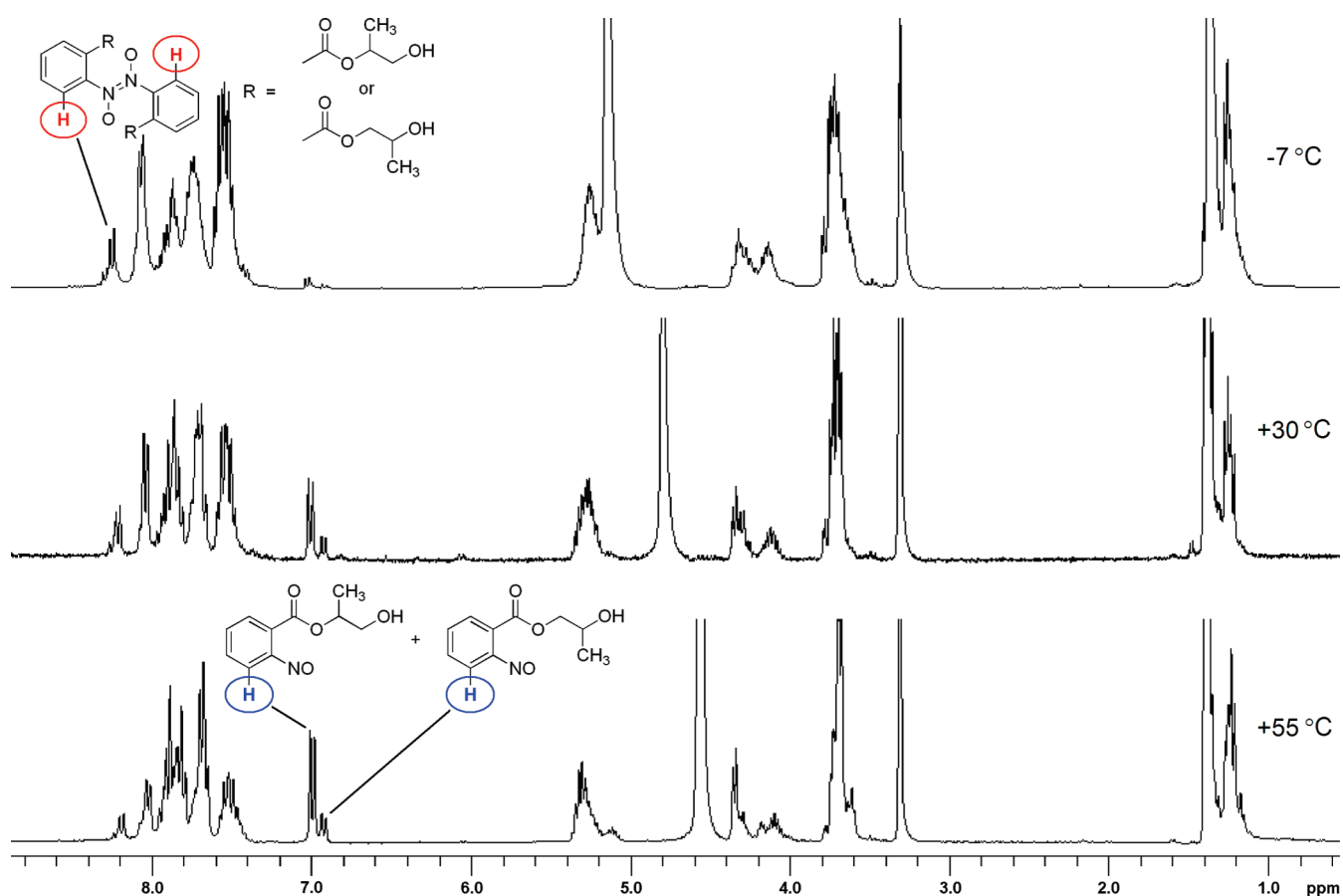
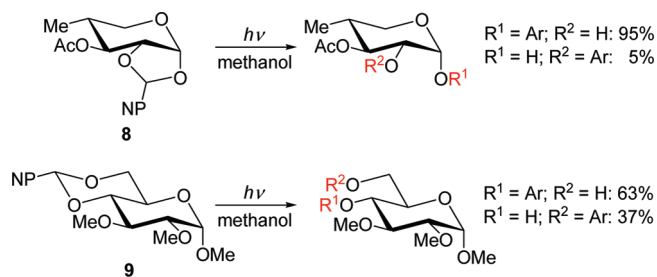


FIGURE 1. Temperature-dependent  $^1\text{H}$  NMR spectra of **2d** in  $\text{CD}_3\text{OD}$ .

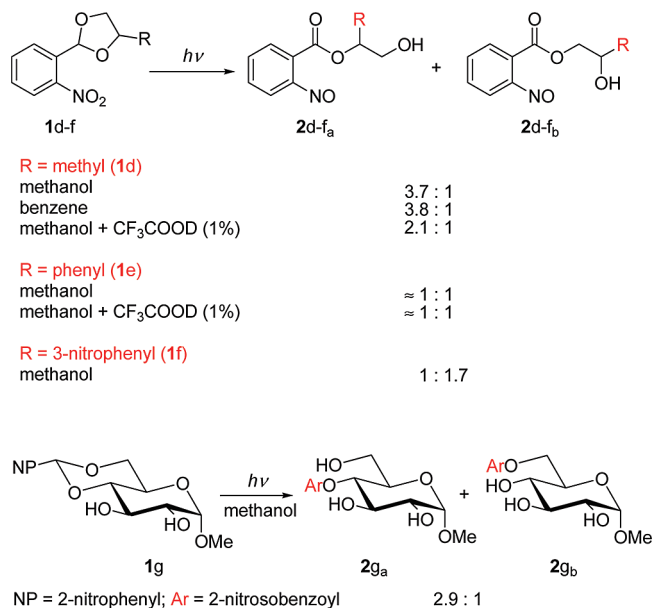
**SCHEME 5. Results from References 22 and 23**



**Computational Studies: Protected Ethan-1,2-diol.** The mechanism of ONB deprotection has also been subject of many studies since its first application as PPG. An archetype compound, 2-nitrotoluene, is known to undergo intramolecular hydrogen shift to form an *aci*-nitro tautomer upon irradiation.<sup>45</sup> This intermediate is a moderately strong acid, and it recovers the ground state of the starting material upon proton tautomerization.<sup>13</sup> It is not clear yet whether the reaction proceeds from the excited singlet or triplet state or both, or whether H-atom transfer and conformational interconversion occur in an electronic excited state. Similar initial steps of the photoreaction have been proposed for various 2-nitrobenzyl moieties substituted in the benzylic position by

(45) Dunkin, I. R.; Gebicki, J.; Kiszka, M.; Sanin-Leira, D. *J. Chem. Soc., Perkin Trans. 2* **2001**, 1414.

**SCHEME 6. Regioselectivity of Photorelease of **2d–g****



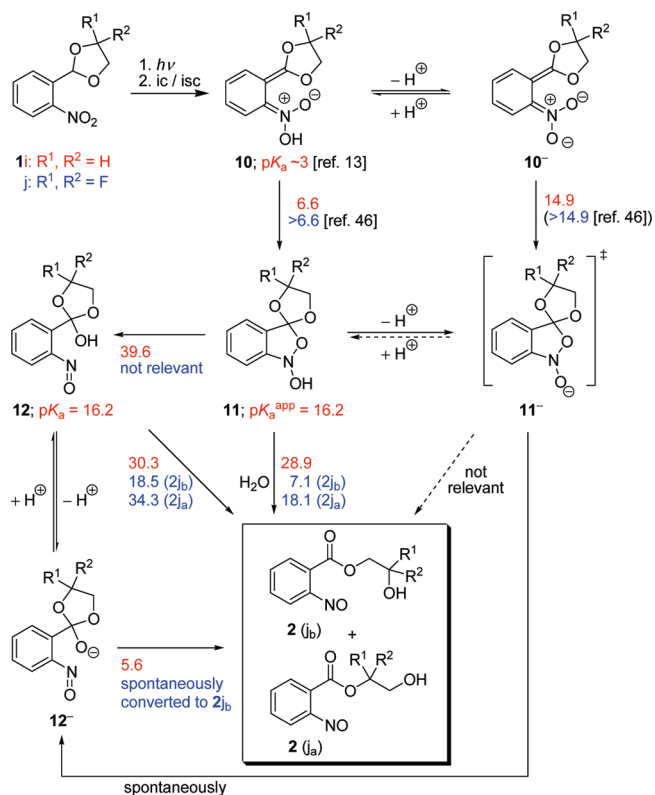
various leaving groups (Scheme 1).<sup>10–18</sup> The decay of the *aci*-nitro intermediates is often taken as the rate-limiting step of the process, and it can proceed via different reaction pathways, the mechanisms of which depend considerably on pH and polarity of a solvent. Although exhaustive computational

studies by Il'ichev and Wirz have been devoted to explaining the experimentally observed trends,<sup>14,15,46,47</sup> the substituent effects on the kinetics of the complete deprotection process remain inadequately understood. None of the previous computational studies included the nitrobenzylidene moiety.

In this work, a series of DFT-based quantum chemical calculations<sup>48</sup> were performed on the reactions of the ethan-1,2-diol derivative **1i**, the simplest model compound, to understand the mechanism of ester **2** formation (Scheme 7; red numbers). Our efforts have been centered on the reaction steps that follow the photochemical formation of the *aci*-nitro intermediate **10** (Scheme 7), which could be decisive in determining the reaction regioselectivity observed. We followed the methodology used previously for rearrangements of 2-nitrobenzyl derivatives using the B3LYP/6-311+G(3df,2p)//B3LYP/6-31G(d) level of theory (with the scaling factor of 0.9613 for vibrational frequencies)<sup>49</sup> to compute activation Gibbs energies ( $\Delta G^\ddagger$ ).<sup>46,47</sup> A polarizable continuum model (PCM) of Tomasi and co-workers was used to mimic the solvation effects on the activation barriers.<sup>50,51</sup> It is known that the B3LYP functional underestimates the activation barriers by more than 3 kcal mol<sup>-1</sup> for most reactions.<sup>52</sup> Hence we considered the B3LYP results to be a lower estimate for the energy requirements of all elementary steps. The structures, total energies (at 0 K), and total Gibbs energies (at 298.15 K) together with Cartesian coordinates for all species considered are given in Supporting Information.

Only the (*E*)-configuration on the C=N bond in **10i** (*trans-aci*-nitro tautomer) was considered because it was more stable than the (*Z*)-isomer by 2.2 kcal mol<sup>-1</sup> (>97.5% *trans-10i*). The subsequent cyclization of **10i** gives the tricyclic *N*-hydroxy-2,3-dihydrobenzo[*d*]isoxazole **11i**. The  $\Delta G^\ddagger$  values of 8.2 kcal mol<sup>-1</sup> in the gas phase and 6.6 kcal mol<sup>-1</sup> in water as an implicit solvent were determined for this process. The *aci*-tautomer is a moderately strong acid ( $pK_a \sim 3.6$  for 2-nitrotoluene<sup>13</sup>) implying a more acidic character of **10i**. The anionic form of **10i**, **10i<sup>-</sup>**, should, therefore, prevail at the neutral pH. Regarding the energy requirements for cyclization (**10i<sup>-</sup>** → **11i<sup>-</sup>**), the Gibbs energy of activation of 17.3 and 14.9 kcal mol<sup>-1</sup> was found in the gas phase and in water, respectively, which is in good agreement with the value calculated by Il'ichev and Wirz for 2-nitrotoluene.<sup>47</sup>

### SCHEME 7. Reaction Mechanism Proposed for **1i** and **1j<sup>a</sup>**



<sup>a</sup>The numbers (red = the reaction of **1i**; blue = the reaction of **1j**) are the activation barriers (in kcal mol<sup>-1</sup>) in water and the pK<sub>a</sub> values.

Three different pathways for **11i** decay were considered. We initially assumed that an equilibrium is established between **11i** and **11i<sup>-</sup>** and that both isomers are formed via ring closure of **10i** or **10i<sup>-</sup>**, respectively. Unfortunately we were unable to locate any minimum which corresponded to **11i<sup>-</sup>**. The optimization process converged to **12i<sup>-</sup>**. The optimization process employing water as a solvent treated as polarizable continuum (PCM) resulted essentially in the same structure. These results suggest that there is a minimal barrier between **11i<sup>-</sup>** and **12i<sup>-</sup>** at both the B3LYP/6-31G(d) and B3LYP/6-31G(d) PCM potential energy surface (PES). This indicates that no equilibrium can be described between **11i** and **11i<sup>-</sup>** because the latter structure decays immediately to **12i<sup>-</sup>**. Therefore, direct conversion of **11i<sup>-</sup>** into the ester of 2-nitrosobenzoic acid **2i** can also be excluded.

It is not surprising that no experimental pK<sub>a</sub> data for compounds analogous to **11i** are available. Previous computational work estimated the gas-phase deprotonation enthalpies of *N*-hydroxy-2,3-dihydrobenzo[*d*]isoxazole derived from 2-nitrotoluene.<sup>47</sup> To estimate a pK<sub>a</sub> of **11i**, we adapted the approach of Pliego and Riveros, predicting the experimental values within 2 pK<sub>a</sub> units,<sup>53</sup> which was previously used in case of 2-nitrobenzyl alcohols.<sup>14</sup> Thus, pK<sub>a</sub><sup>app</sup> = 16.2 (app = apparent) was calculated for **11i**. In addition, **11i** can also form **12i** via an intramolecular proton transfer (or [1,3]-H shift) from *N*-hydroxy group to the oxygen on the 2,3-dihydrobenzo[*d*]isoxazole ring, followed by the ring-opening. The gas-phase  $\Delta G^\ddagger$  of 38.3 kcal mol<sup>-1</sup> was found for this

(46) Il'ichev, Y. V. *J. Phys. Chem. A* **2003**, *107*, 10159.

(47) Il'ichev, Y. V.; Wirz, J. *J. Phys. Chem. A* **2000**, *104*, 7856.

(48) Frisch, M. J.; Trucks, G. W.; Schlegel, H. B.; Scuseria, G. E.; Robb, M. A.; Cheeseman, J. R.; Montgomery, J. A., Jr.; Kudin, T. V. K. N.; Burant, J. C.; Millam, J. M.; Iyengar, S. S.; Tomasi, J.; Barone, V.; Mennucci, B.; Cossi, M.; Scalmani, G.; Rega, N.; Petersson, G. A.; Nakatsuji, H.; Hada, M.; Ehara, M.; Toyota, K.; Fukuda, R.; Hasegawa, J.; Ishida, M.; Nakajima, T.; Honda, Y.; Kitao, O.; Nakai, H.; Klene, M.; Li, X.; Knox, J. E.; Hratchian, H. P.; Cross, J. B.; Adamo, C.; Jaramillo, J.; Gomperts, R.; Stratmann, R. E.; Yazyev, O.; Austin, A. J.; Cammi, R.; Pomelli, C.; Ochterski, J. W.; Ayala, P. Y.; Morokuma, K.; Voth, G. A.; Salvador, P.; Dannenberg, J. J.; Zakrzewski, G.; Dapprich, S.; Daniels, A. D.; Strain, M. C.; Farkas, O.; Malick, D. K.; Rabuck, A. D.; Raghavachari, K.; Foresman, J. B.; Ortiz, J. V.; Cui, Q.; Baboul, A. G.; Clifford, S.; Cioslowski, M. J.; Stefanov, B. B.; Liu, G.; Liashenko, A.; Piskorz, P.; Komaromi, I.; Martin, R. L.; Fox, D. J.; Keith, T.; Al-Laham, M. A.; Peng, C. Y.; Nanayakkara, A.; Challacombe, M.; Gill, P. M. W.; Johnson, B.; Chen, W.; Wong, M. W.; Gonzalez, C.; Pople, J. A. *Gaussian 03*; Gaussian, Inc.: Pittsburgh, PA, 2003.

(49) Merrick, J. P.; Moran, D.; Radom, L. *J. Phys. Chem. A* **2007**, *111*, 11683.

(50) Cossi, M.; Barone, V.; Cammi, R.; Tomasi, J. *Chem. Phys. Lett.* **1996**, *255*, 327.

(51) Miertus, S.; Scrocco, E.; Tomasi, J. *Chem. Phys.* **1981**, *55*, 117.

(52) Boese, A. D.; Martin, J. M. L. *J. Chem. Phys.* **2004**, *121*, 3405.

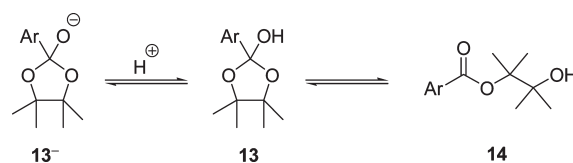
(53) Pliego, J. R.; Riveros, J. M. *J. Phys. Chem. A* **2002**, *106*, 7434.

process, which is considerably smaller than that reported for 2-nitrotoluene derivatives.<sup>47</sup> The solvation showed only a negligible effect on the barrier; its value increased only to 39.6 kcal mol<sup>-1</sup> when water was included. We also performed additional proton transfer to **11i** that might lead directly to **2**. We assumed that the proton from the *N*-hydroxy group could be transferred to one of the oxygen atoms belonging to the protected diol. However, it made no sense to optimize such a process in silico because the charge separation would lead to exceedingly high energies. Instead, an explicit molecule of water, which served as a proton carrier, was employed. We were able to locate a transition state TS[**11i** → **2i**] that corresponded to a one-step transformation of **11i** to the ester of 2-nitrobenzoic acid (**2**). The comparable and relatively high  $\Delta G^\ddagger$  of 24.3 and 28.9 kcal mol<sup>-1</sup> were found for the reaction in the gas phase and water environment, respectively.

The final step in the mechanism shown in Scheme 7 is the transformation of the hemioortho ester **12i** or its anionic form **12i**<sup>-</sup> to **2**. Two transition states with stable restricted wave functions for **12i** decay, differing by the angle contained between the hemioortho ester hydroxy group and the benzene ring, were found. The 30.1 and 31.3 kcal mol<sup>-1</sup> values of  $\Delta G^\ddagger$  in the gas phase were obtained, while the energy in the water environment changed slightly to 30.3 kcal mol<sup>-1</sup> and 30.9 kcal mol<sup>-1</sup>, respectively. A single transition state was located for **12i**<sup>-</sup> (TS[**12i**<sup>-</sup> → **2i**<sup>-</sup>]). The computed  $\Delta G^\ddagger$  of 3.4 and 5.6 kcal mol<sup>-1</sup> were obtained in the gas phase and water, respectively. Both **12i** and **12i**<sup>-</sup> are in equilibrium. The p*K*<sub>a</sub> values between 11 and 12 have already been reported for common hemioortho esters.<sup>54</sup> Here we used the method of Riveros and Pliego<sup>53</sup> to estimate the p*K*<sub>a</sub> of **12i** to obtain the value of ~16 again. However, we assume that the authentic value should be lower by several p*K*<sub>a</sub> units. McClelland and co-workers described the hemioortho ester anion **13**<sup>-</sup> to be in equilibrium with its ring-opened form **14** (Scheme 8) and reported p*K*<sub>a</sub> of ~10 for the neutral hemioortho ester **13**.<sup>55</sup>

A profile of the potential energy surface calculated for the phototransformation of **1i** is lucidly depicted in Figures 2 (neutral form) and 3 (deprotonated form). The Gibbs energies for various intermediates and transition states are given relative to *trans*-**10i** and **10i**<sup>-</sup>. The *aci*-nitro derivative *trans*-**10i** cyclizes into **11i** (or **11i**<sub>w</sub>, with an explicit molecule of water) with relatively low barrier of 6.6 kcal mol<sup>-1</sup>. The anion **10i**<sup>-</sup> possesses a considerably higher barrier for cyclization (14.9 kcal mol<sup>-1</sup> in water). Since *aci*-nitro intermediates are moderately strong acids (p*K*<sub>a</sub> ~3.6 for 2-nitrotoluene<sup>13</sup>), acid catalysis is expected to occur in this step even at neutral pH. Three alternatives are possible for **11i** decay. Nevertheless, it is clear that the reaction barriers connecting **11i** (or **11i**<sub>w</sub>) with **12i**<sub>b</sub> (or **2** directly) are very high. The last pathway considered involved the deprotonation of **11i** to give a hypothetical species **11i**<sup>-</sup>, which is transformed spontaneously to **12i**<sup>-</sup>. Base catalysis is essential for this step. **12i** is a relatively weak acid that prefers a neutral form; therefore, we suggest that base catalysis is a part of decay of the hemioortho ester **12i**.

SCHEME 8



**Computational Studies: Protected Substituted Nonsymmetric Ethan-1,2-diols.** Hypothetical 1,1-difluoroethan-1,2-diol (**1j**) was investigated by the same methods as those described in the previous paragraph in order to explain the acetal C–O bond cleavage priority in nonsymmetric 1,2-diols. It was assumed that a strong inductive effect of the fluorine atoms should considerably change the reactivity of the key intermediates. The substituent effects on the *aci*-nitro intermediates cyclization have been previously studied computationally.<sup>46</sup> We located two transition states TS[**11j**<sub>wa</sub> → **2j**<sub>a</sub>] and TS[**11j**<sub>wb</sub> → **2j**<sub>b</sub>] (for indexes, see Supporting Information, page S10), the activation energies of which, 18.1 and 7.1 kcal mol<sup>-1</sup>, respectively, clearly suggest that the cleavage of the C–O bond with the neighboring fluorine substitution is largely favored (Scheme 7). The effect of fluorine atoms on the transformation is enormous when compared to the results for **11i**. It is reasonable to assume that the p*K*<sub>a</sub> for **11j** will drop below that of **11i** as a result of the strong inductive effect of fluorine atoms.

In addition, we explored the impact of this substitution on the last reaction step, a decay of **12j**. Two transition states leading to each of the isomeric esters were located. The cleavage of the C–OCF<sub>2</sub> bond possessed a lower barrier of 18.5 kcal mol<sup>-1</sup> (TS[**12j** → **2j**<sub>b</sub>]) in water compared to that of 34.3 kcal mol<sup>-1</sup> (TS[**12j** → **2j**<sub>a</sub>]). **12j**<sup>-</sup> was affected by the substitution even more. The optimization process exclusively converged to a structure reminiscent of **2j**<sub>b</sub> (Scheme 9). We tried to include the solvent or change the basis set by adding diffuse functions (6-31+G\*) in this optimization procedure with the same conclusion.

Finally, we wished to confirm our experimental results obtained from the HMBC spectra analyses of **2d**<sub>a</sub> (major) and **2d**<sub>b</sub> (minor) formation (Scheme 6). The observed (experimental) ratio of 3.7 corresponds to an activation energy difference of less than 1 kcal mol<sup>-1</sup> at 298 K. It is clear that such small energy differences are on the edge of the DFT performance; therefore, it cannot provide fully convincing results. In addition, a stereogenic center in the molecule of a nonsymmetric diol introduces a large amount of various diastereomers essentially in each step of the reaction mechanism. Modeling such a reaction mechanism is thus exceedingly complex.

Nevertheless, here we considered the cyclization of the *aci*-nitro form of all possible **10d** diastereomers (the (*E*)-configuration of the C=N bond of the former nitro group was assumed). All four species were found to be similar in energy. The activation Gibbs energies varied only by 1.7 kcal mol<sup>-1</sup> (see Table SI-3 and Figure SI-18 in Supporting Information). None of the reactions was energetically disfavored and the cyclization proceeded from all four diastereomers. We then focused on the last step in the transformation, the dioxolane ring opening in the hemioortho ester **12d** or its anionic form **12d**<sup>-</sup>. We were able to locate eight transition states with stable restricted wave function for diastereomers of **12d**

(54) Guthrie, J. P. *J. Am. Chem. Soc.* **1978**, *100*, 5892.

(55) McClelland, R. A.; Santry, L. J. *Acc. Chem. Res.* **1983**, *16*, 394.

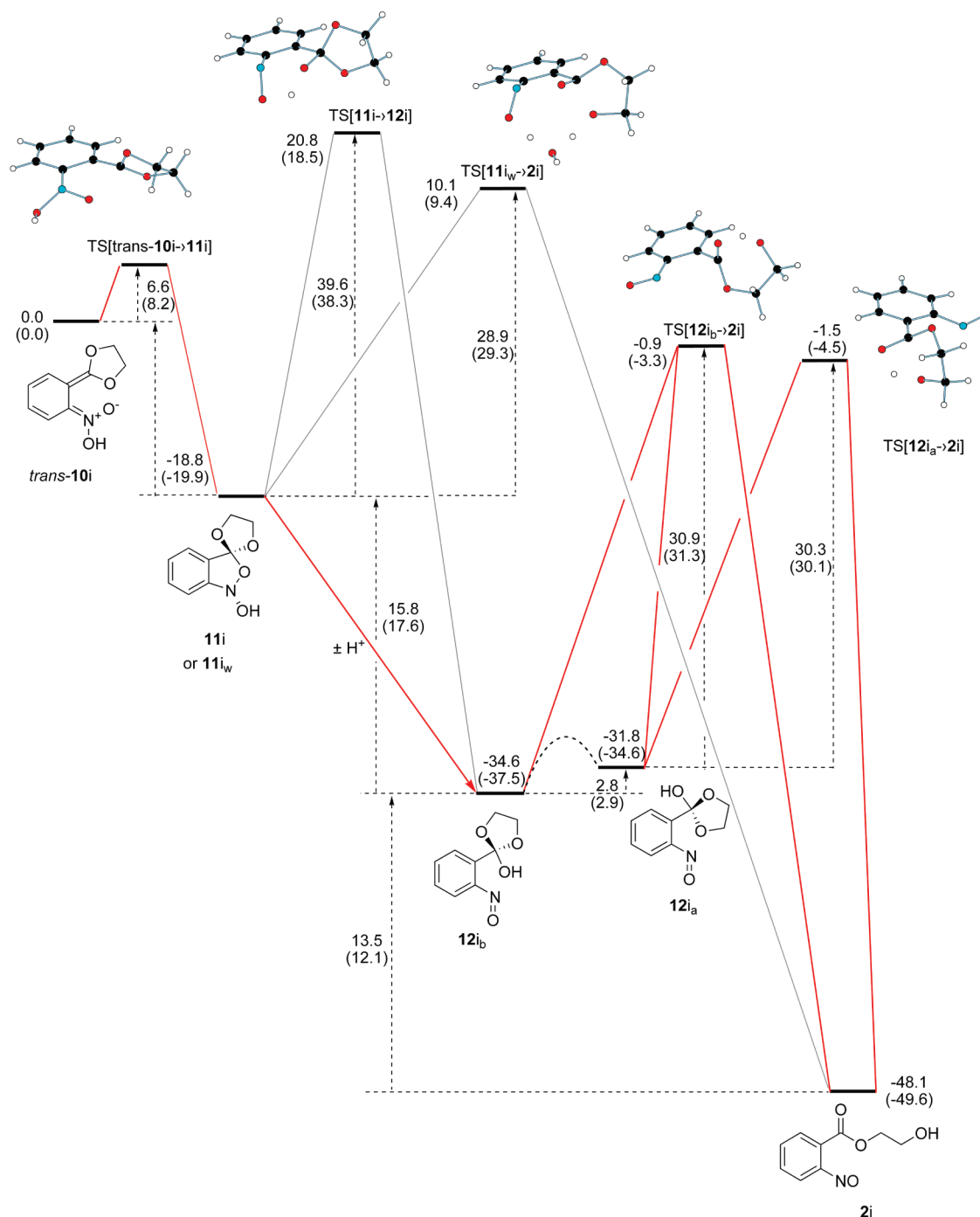


**FIGURE 2.** Profile of the potential energy surface for the transformation of the *aci*-nitro moiety **10i** into **2i**. The subscript (<sub>w</sub>) denotes an explicit water molecule used in the calculation. Gibbs energies in water relative to *trans-10i* are given in kcal mol<sup>-1</sup>. The values relevant for the gas phase are in parentheses. The barriers and the reaction energies for individual steps are shown near the corresponding dashed arrows. Red color is used to highlight the preferred steps.

(two TS for each diastereomer). The results obtained preclude creating a complete and all-inclusive picture of the observed regioselectivity as expected. However, we would like to illustrate that the energy differences in the activation barriers are so small that the **2d<sub>a</sub>**/**2d<sub>b</sub>** ratio must be close to 1. The transition states and their energies are listed in Figure SI-19 and Table SI-4 in Supporting Information.

We located two transition states for each of the **12d<sup>-</sup>** diastereomers (**12d<sup>-</sup>** → **2d<sub>a</sub>** or **2d<sub>b</sub>**). However, they do not

interconnect the lowest energy minima with those of the products. The transition states and their energies are summarized in Figure SI-20, Figure SI-21, and Table SI-5 in Supporting Information. The results suggest that each diastereomer prefers formation of a different regioisomer of the product. Hence the final product ratio could be affected by another slow step in the mechanism, that is, by the rates of the diastereomers **12d<sup>-</sup>** formation. A similar trend can be found for the neutral form **12d**.



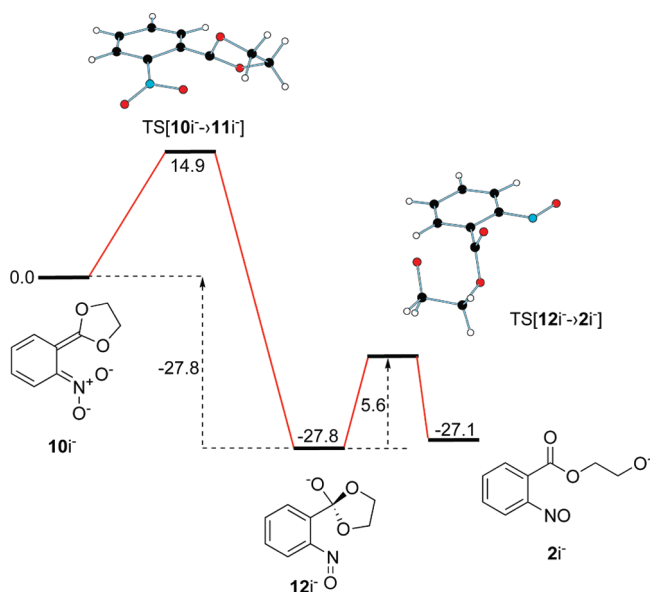
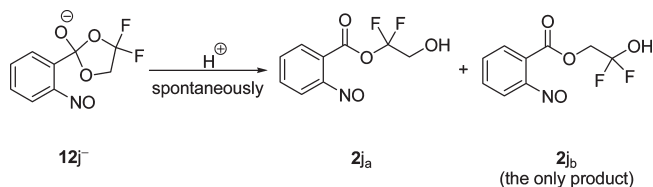


**FIGURE 3.** Profile of the potential energy surface for the transformation of the *aci*-nitro moiety  $10i^-$  into  $2i^-$ . The Gibbs energies in water relative to  $10i^-$  are given in  $\text{kcal mol}^{-1}$ . The barriers and reaction energies for individual steps are shown near the corresponding dashed arrows.

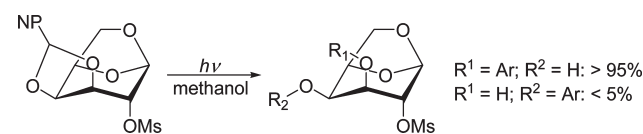
#### SCHEME 9



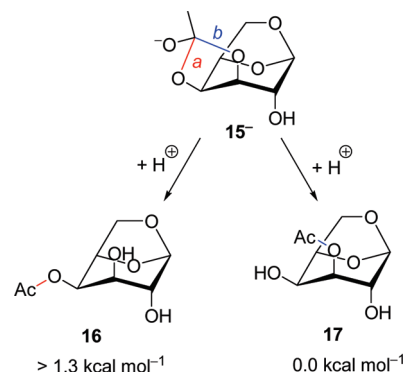
We have already shown that the regioselectivity of the acetal cleavage in nonsymmetric ONBA derivatives, such as **1d** or **1j**, is, in principle, based on the leaving ability evaluation of one of the terminal groups, although steric effects should not be neglected. However, such a simple model cannot unequivocally explain the regioselectivity observed in some carbohydrate derivatives,<sup>23</sup> such as **9** in Scheme 5.

To study a similar ONB structure, such as an acetal shown in Scheme 10 previously studied by Collins,<sup>22</sup> we selected a model compound **15** (Scheme 11). We found that the two *endo* C–O bonds of a hemioortho ester group in  $15^-$  differ significantly in length. The *a* versus *b* length difference of 0.154 Å was obtained using the B3LYP/6-31G(d) level of theory. Improving the basis set by adding diffuse (6-31+G(d)) and polarization (6-31+G(d,p)) functions reduced the difference to 0.104 and 0.105 Å, respectively. It appeared that the solvation plays an important role here. The B3LYP/6-31+G(d) geometry with PCM solvation model of water further attenuated the difference to 0.039 Å. However, we faced a problem with the convergence criteria in this case, and hence we performed an MP2/6-31+G(d) geometry optimization to obtain the same result with the difference of 0.066 Å. All these findings suggest that the regioselectivity in the  $15^-$  decay should be observed experimentally and they indeed agree with the observation of Collins and co-workers depicted in Scheme 10.

#### SCHEME 10. Data from Reference 22



#### SCHEME 11. Decay of $15^-$

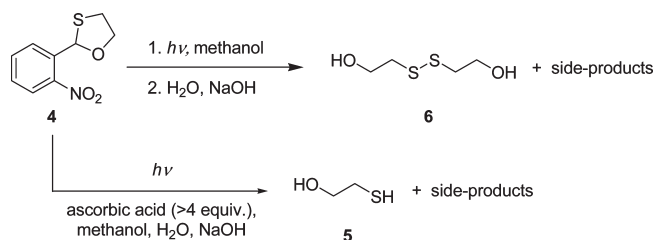


*endo* C–O bonds highlighted in red (bond *a*) and blue (bond *b*). The relative Gibbs energies for **16** and **17** are shown.

In addition, our calculations predicted that **17** was lower in energy by at least 1.3  $\text{kcal mol}^{-1}$  relative to the optimized conformers of **16** (Scheme 11) at the B3LYP/6-311+G(2d, p)//B3LYP/6-31G(d) level of theory. It suggests that more strain energy of the five-membered ring in  $15^-$  is released when  $15^-$  decays to **17**, and it is in agreement with the results of Collins and co-workers. Note that **2d<sub>a</sub>** (major) and **2d<sub>b</sub>** (minor) were found equal in energy within 0.1  $\text{kcal mol}^{-1}$  (the experimental ratio is 3.7:1 in methanol).

**Photolysis of Monothioacetal 4.** Photolysis of the monothioacetal **4** in methanol followed by basic hydrolysis resulted in high yields of bis(2-hydroxyethyl) disulfide (**6**; Scheme 12; Table 1) instead of 2-thioethanol (**5**). In contrast, **5** was obtained in approximately 90% chemical yield when **4** was irradiated in the presence of more than 4 equiv of ascorbic acid, a frequently employed reducing agent,<sup>56,57</sup> following both stepwise and one-pot deprotection protocols (Table 1). Both photoproducts were easily identified by <sup>1</sup>H NMR in situ thanks to the characteristic  $-\text{CH}_2\text{SH}$  versus  $-(\text{CH}_2)\text{S}-\text{S}(\text{CH}_2)-$  peaks.

#### SCHEME 12

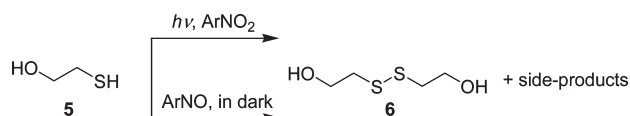


(56) Hamada, T.; Nishida, A.; Yonemitsu, O. *J. Am. Chem. Soc.* **1986**, *108*, 140.

(57) Liu, Q.; Han, B.; Liu, Z. G.; Yang, L.; Liu, Z. L.; Yu, W. *Tetrahedron Lett.* **2006**, *47*, 1805.

The formation of **6** was explored. 2-Thioethanol was found to be photostable in methanol as well as in methanol containing NaOH (0.2 M) even when purged with O<sub>2</sub> in dark. On the other hand, bis(2-hydroxyethyl) disulfide (**6**) was formed in the presence of nitrobenzene in methanol under irradiation (> 280 nm, Pyrex filter; nitrobenzene itself is not photoreduced in methanol under these conditions) as well as in the presence of 2-nitrosobenzoic acid<sup>16,58</sup> (Scheme 13) in dark. Therefore, both photooxidation by the starting nitrobenzyl acetal and oxidation by the nitroso intermediate formed in the first step of photochemical deprotection could be responsible for oxidative formation of a disulfide from a thiol.

#### SCHEME 13



#### Conclusions

Chemically stable and synthetically accessible 2-nitrobenzylidene acetals (ONBA) can be utilized for protection of dihydroxy compounds. The substrates are released in two reactions: (1) a photochemical transformation to the 2-nitrosobenzoic acid esters, and (2) their subsequent acid- or base-catalyzed hydrolysis to yield the diol. Here we report that substrates are liberated in excellent chemical yields by a one-pot procedure that includes both steps. The study also explored the scope and limitations of ONBA photochemistry, in particular, that of nonsymmetrically substituted acetals preferentially yielding the esters with moderate to high regioselectivity. Both the experimental data and DFT-based quantum chemical calculations favored preferential cleavage of the acetal C–O bond in the vicinity of a more electron-withdrawing (or a less electron-donating) group, which reflects the better leaving-group ability of the corresponding hydroxy group. The release mechanism involves a very complex sequence through the *aci*-nitro intermediate **10** on to the 2,3-dihydrobenzo[*d*]isoxazole intermediate **11** and ultimately to the hemioortho ester **12**. Structural variations of the substrate will influence the partitioning of these intermediates and will alter the ratios of the hydroxyester photoproduct mixture for unsymmetrical acetals. Similar deprotection strategy was also applied for 2-thioethanol when released from the corresponding monothioacetal in the presence of a reducing agent.

#### Experimental Section

**General Procedure for the Synthesis of Acetals 1a–f and Monothioacetal 4.** A solution of a dihydroxy compound (**3a–f**; 7.2 mmol) or 2-thioethanol (**5**, 7.2 mmol), 2-nitrobenzaldehyde (7.2 mmol), and *p*-toluene sulfonic acid (PTSA; 0.5 mmol) in toluene (150 mL) was refluxed under Dean–Stark conditions until the starting material disappeared (TLC), usually for 4–10 h. The reaction mixture was then washed with aqueous NaOH (40 mL; 10%) and water (2 × 50 mL), dried over MgSO<sub>4</sub>, and the solvent was removed under reduced pressure. The crude product was purified by flash chromatography.

(58) Schaper, K. *Magn. Reson. Chem.* **2008**, *46*, 1163.

**trans-Hexahydro-2-(2-nitrophenyl)benzo[*d*][1,3]dioxole (1a).** Prepared from **3a** in 93% yield; light yellow viscous liquid. <sup>1</sup>H NMR (300 MHz, CDCl<sub>3</sub>): δ (ppm) 1.19–1.37 (m, 2H), 1.52 (dt, 2H, *J*<sub>1</sub> = 11.0 Hz, *J*<sub>2</sub> = 2 Hz), 1.85 (dd, 2H, *J*<sub>1</sub> = 11.0 Hz), 2.14–2.28 (m, 2H), 3.16–3.25 (m, 1H), 3.41–3.50 (m, 1H), 6.67 (s, 1H), 7.49 (dt, 1H, *J*<sub>1</sub> = 7.8 Hz, *J*<sub>2</sub> = 1.2 Hz), 7.63 (dt, 1H, *J*<sub>1</sub> = 7.6 Hz, *J*<sub>2</sub> = 1.0 Hz), 7.86 (dd, 1H, *J*<sub>1</sub> = 8.0 Hz, *J*<sub>2</sub> = 1.3 Hz), 7.93 (dd, 1H, *J*<sub>1</sub> = 8.3 Hz, *J*<sub>2</sub> = 1.0 Hz). <sup>13</sup>C NMR (75.5 MHz, CDCl<sub>3</sub>): δ (ppm) 23.3; 23.4; 28.4; 28.5; 79.7; 82.1; 98.9; 124.1; 127.3; 129.2; 132.7; 134.2; 148.5. MS (EI, *m/z*): 248, 232, 151, 134, 121, 104, 97, 79, 69, 51, 41. FTIR (KBr, cm<sup>-1</sup>): 3476, 3414, 2945, 2868, 1528, 1348, 1113, 1072, 963, 855, 749, 627. UV–vis: ε<sub>313</sub> (acetonitrile) = 680 dm<sup>3</sup> mol<sup>-1</sup> cm<sup>-1</sup>; ε<sub>366</sub> (acetonitrile) = 180 dm<sup>3</sup> mol<sup>-1</sup> cm<sup>-1</sup>; ε<sub>313</sub> (MeOH) = 700 dm<sup>3</sup> mol<sup>-1</sup> cm<sup>-1</sup>; ε<sub>366</sub> (MeOH) = 190 dm<sup>3</sup> mol<sup>-1</sup> cm<sup>-1</sup>; ε<sub>313</sub> (cyclohexane) = 440 dm<sup>3</sup> mol<sup>-1</sup> cm<sup>-1</sup>; ε<sub>366</sub> (cyclohexane) = 150 dm<sup>3</sup> mol<sup>-1</sup> cm<sup>-1</sup>. HRMS (EI+) for C<sub>13</sub>H<sub>15</sub>NO<sub>4</sub> (M<sup>+</sup>) 249.1001, found 249.1017.

**cis-Hexahydro-2-(2-nitrophenyl)benzo[*d*][1,3]dioxole (1b).** Prepared from **3b** in 95% yield; slightly yellow crystals. Mp 44.5–46.0 °C. <sup>1</sup>H NMR (300 MHz, CDCl<sub>3</sub>): δ (ppm) 1.25–1.37 (m, 2H), 1.55–1.68 (m, 2H), 1.70–1.94 (m, 4H), 4.10 (p, 2H, *J* = 4.6 Hz), 6.75 (s, 1H), 7.47 (dt, 1H, *J*<sub>1</sub> = 7.9 Hz, *J*<sub>2</sub> = 1.3 Hz), 7.60 (t, 1H, *J* = 7.2 Hz), 7.79 (d, 1H, *J* = 7.8 Hz), 7.88 (d, 1H, *J* = 8.0 Hz) (diastereomer a; isolated); 1.25–1.38 (m, 2H), 1.46–1.57 (m, 2H), 1.72–1.81 (m, 4H), 4.22 (p, 2H, *J* = 5.1 Hz), 6.44 (s, 1H), 7.50 (t, 1H, *J* = 7.8 Hz), 7.65 (t, 1H, *J* = 7.6 Hz), 7.98 (d, 1H, *J* = 7.8 Hz), 7.92 (d, 1H, *J* = 8.1 Hz) (diastereomer b; isolated). <sup>13</sup>C NMR (75.5 MHz, CDCl<sub>3</sub>): δ (ppm) 20.8, 28.1, 75.1, 98.5, 124.2, 127.6, 129.5, 132.9, 134.0, 148.8 (diastereomer a) 20.9, 27.2, 74.5, 98.2, 124.4, 127.4, 129.2, 132.7, 135.2, 148.8 (diastereomer b). MS (EI, *m/z*): 248, 232, 150, 134, 121, 104, 91, 81, 69, 51, 41. FTIR (KBr, cm<sup>-1</sup>): 3425, 2937, 2864, 1533, 1448, 1367, 1209, 1105, 1068, 999, 786, 730. UV–vis: ε<sub>313</sub> (MeOH) = 650 dm<sup>3</sup> mol<sup>-1</sup> cm<sup>-1</sup>, ε<sub>366</sub> (MeOH) = 190 dm<sup>3</sup> mol<sup>-1</sup> cm<sup>-1</sup>, ε<sub>313</sub> (cyclohexane) = 400 dm<sup>3</sup> mol<sup>-1</sup> cm<sup>-1</sup>, ε<sub>366</sub> (cyclohexane) = 150 dm<sup>3</sup> mol<sup>-1</sup> cm<sup>-1</sup>. Anal. Calcd for C<sub>13</sub>H<sub>15</sub>NO<sub>4</sub>: C, 62.64; H, 6.07; N, 5.62. Found: C, 62.62; H, 6.10; N, 5.62.

**3-(2-Nitrophenyl)-2,4-dioxabicyclo[3.3.1]nonane (1c).** Prepared from **3c** in 95% yield; yellowish crystals. Mp 32–35 °C. <sup>1</sup>H NMR (300 MHz, CDCl<sub>3</sub>): δ (ppm) 1.33–1.52 (m, 4H), 1.86–1.94 (m, 2H), 2.09–2.23 (m, 1H), 2.71–2.81 (m, 1H), 4.48 (t, 2H, *J* = 3.4 Hz), 6.63 (s, 1H), 7.42 (dt, 1H, *J*<sub>1</sub> = 7.8 Hz, *J*<sub>2</sub> = 1.4 Hz), 7.59 (t, 1H, *J* = 7.6 Hz), 7.77 (dd, 1H, *J*<sub>1</sub> = 8.1 Hz, *J*<sub>2</sub> = 0.9 Hz), 8.00 (dd, 1H, *J*<sub>1</sub> = 7.9 Hz, *J*<sub>2</sub> = 0.9 Hz). <sup>13</sup>C NMR (75.5 MHz, CDCl<sub>3</sub>): δ (ppm) 16.0; 27.8; 32.2; 69.5; 86.8; 123.9; 128.4; 129.2; 132.8; 133.5; 148.6. MS (EI, *m/z*): 248, 232, 152, 134, 121, 104, 93, 81, 65, 51, 41. FTIR (KBr, cm<sup>-1</sup>): 3396, 3301, 2935, 2859, 1529, 1450, 1349, 1192, 1130, 1010, 786, 740. UV–vis: ε<sub>313</sub> (MeOH) = 600 dm<sup>3</sup> mol<sup>-1</sup> cm<sup>-1</sup>, ε<sub>366</sub> (MeOH) = 190 dm<sup>3</sup> mol<sup>-1</sup> cm<sup>-1</sup>, ε<sub>313</sub> (cyclohexane) = 410 dm<sup>3</sup> mol<sup>-1</sup> cm<sup>-1</sup>, ε<sub>366</sub> (cyclohexane) = 160 dm<sup>3</sup> mol<sup>-1</sup> cm<sup>-1</sup>. Anal. Calcd for C<sub>13</sub>H<sub>15</sub>NO<sub>4</sub>: C, 62.64; H, 6.07; N, 5.62. Found: C, 62.77; H, 6.13; N, 5.52.

**4-Methyl-2-(2-nitrophenyl)-1,3-dioxolane (1d).** Prepared from **3d** in 88% yield; yellowish oil. <sup>1</sup>H NMR (300 MHz, CDCl<sub>3</sub>): δ (ppm) 1.28 (m, 6H), 3.36–3.56 (m, 2H), 4.00–4.14 (m, 2H), 4.20 (td, 1H, *J*<sub>1</sub> = 5.9 Hz, *J*<sub>2</sub> = 11.9 Hz), 4.32 (td, 1H, *J*<sub>1</sub> = 6.1 Hz, *J*<sub>2</sub> = 6.8 Hz), 6.36 (s, 1H), 6.56 (s, 1H), 7.37–7.49 (m, 2H), 7.51–7.62 (m, 2H), 7.68–7.87 (m, 4H); a mixture of two diastereomers). <sup>13</sup>C NMR (75.5 MHz, CDCl<sub>3</sub>): δ (ppm) 17.9; 18.0; 71.2; 71.6; 72.5; 73.8; 99.2; 99.4; 124.1; 124.3; 127.5; 127.9; 129.5; 129.6; 132.7; 132.9; 133.2; 133.7; 133.8; 134.0; 148.7; 148.8. MS (EI, *m/z*): 208, 192, 162, 150, 135, 121, 104, 91, 79, 59, 51, 41. FTIR (KBr, cm<sup>-1</sup>): 2977, 2883, 1702, 1531, 1531, 1201, 1105, 1065, 730. UV–vis: ε<sub>313</sub> (MeOH) = 600 dm<sup>3</sup> mol<sup>-1</sup> cm<sup>-1</sup>, ε<sub>366</sub> (MeOH) = 200 dm<sup>3</sup> mol<sup>-1</sup> cm<sup>-1</sup>, ε<sub>313</sub> (cyclohexane) = 400 dm<sup>3</sup> mol<sup>-1</sup> cm<sup>-1</sup>,

$\epsilon_{366}$  (cyclohexane) = 140 dm<sup>3</sup> mol<sup>-1</sup> cm<sup>-1</sup>. HRMS (EI+) for C<sub>10</sub>H<sub>11</sub>NO<sub>4</sub> (M<sup>+</sup>) 209.0688, found 209.0682.

**2-(2-Nitrophenyl)-4-phenyl-1,3-dioxolane (1e).** Prepared from **3e** in 95% yield; light yellow oil. <sup>1</sup>H NMR (300 MHz, CDCl<sub>3</sub>):  $\delta$  (ppm) 3.86 (td, 2H,  $J_1 = 7.8$  Hz,  $J_2 = 11.9$  Hz), 4.41 (m, 2H), 5.14 (m, 1H), 5.23 (t, 1H,  $J = 7.0$  Hz), 6.63 (s, 1H), 6.85 (s, 1H), 7.38 (m, 10H), 7.53 (m, 2H), 7.65 (t, 2H,  $J = 7.5$  Hz), 7.95 (td, 4H,  $J_1 = 9.2$  Hz,  $J_2 = 16.9$  Hz) (a mixture of two diastereomers). <sup>13</sup>C NMR (75.5 MHz, CDCl<sub>3</sub>):  $\delta$  (ppm) 71.8; 72.5; 77.9; 79.1; 100.0; 100.4; 124.3; 124.4; 125.9; 126.3; 127.5; 127.7; 128.2; 128.3; 128.5; 128.6; 129.6; 129.7; 132.8; 132.9; 138.1; 138.6. MS (EI,  $m/z$ ): 269, 208, 165, 150, 135, 119, 104, 91, 79, 65, 51. FTIR (KBr, cm<sup>-1</sup>): 3064, 3033, 2941, 2887, 1955, 1734, 1529, 1352, 1107, 1066, 698. UV-vis:  $\epsilon_{313}$  (MeOH) = 1000 dm<sup>3</sup> mol<sup>-1</sup> cm<sup>-1</sup>,  $\epsilon_{366}$  (MeOH) = 300 dm<sup>3</sup> mol<sup>-1</sup> cm<sup>-1</sup>,  $\epsilon_{313}$  (cyclohexane) = 720 dm<sup>3</sup> mol<sup>-1</sup> cm<sup>-1</sup>,  $\epsilon_{366}$  (cyclohexane) = 250 dm<sup>3</sup> mol<sup>-1</sup> cm<sup>-1</sup>. HRMS (EI+) for C<sub>15</sub>H<sub>13</sub>NO<sub>4</sub> (M<sup>+</sup>) 271.0845, found 271.0846.

**2-(2-Nitrophenyl)-4-(3-nitrophenyl)-1,3-dioxolane (1f).** Prepared from **3f** in 94% yield; yellowish crystals. Mp 62.5–67 °C. <sup>1</sup>H NMR (300 MHz, CDCl<sub>3</sub>):  $\delta$  (ppm) 3.91 (dd, 1H,  $J_1 = 8.1$  Hz,  $J_2 = 6.4$  Hz), 4.49 (d, 1H,  $J_1 = 8.1$  Hz,  $J_2 = 7.1$  Hz), 5.35 (t, 1H,  $J = 6.8$  Hz), 6.65 (s, 1H), 7.54 (m, 1H), 7.61 (dd, 1H,  $J_1 = 7.8$  Hz,  $J_2 = 1.2$  Hz), 7.65 (d, 1H,  $J = 7.9$  Hz), 7.71 (t, 1H,  $J = 7.8$  Hz), 7.96 (d, 1H,  $J = 8.9$  Hz), 7.99 (d, 1H,  $J = 7.9$  Hz) 8.16 (m, 2H) (diastereomer a). 3.90 (dd, 1H,  $J = 8.3$  Hz), 4.49 (dd, 1H,  $J_1 = 8.4$  Hz,  $J_2 = 6.4$  Hz), 5.25 (t, 1H,  $J = 6.8$  Hz), 6.89 (s, 1H), 7.60 (m, 2H), 7.69 (t, 1H,  $J = 7.4$  Hz), 7.79 (d, 1H,  $J = 7.9$  Hz), 7.89 (dd, 1H,  $J_1 = 8.1$  Hz,  $J_2 = 0.5$  Hz), 7.97 (dd, 1H,  $J_1 = 7.4$  Hz,  $J_2 = 0.5$  Hz), 8.20 (d, 1H,  $J = 7.3$  Hz), 8.25 (s, 1H) (diastereomer b). <sup>13</sup>C NMR (75.5 MHz, CDCl<sub>3</sub>):  $\delta$  (ppm) 72.1; 78.0; 100.8; 121.6; 123.4; 124.8; 127.8; 129.9; 130.3; 132.1; 132.5; 133.4; 141.3; 148.6; 163.3 (diastereomer a). 72.4; 77.1; 101.1; 121.2; 123.4; 124.9; 127.7; 130.2; 132.1; 133.0; 133.2; 141.5; 148.7 (diastereomer b). MS (EI,  $m/z$ ): 316 (M<sup>+</sup>), 299, 269, 166, 149, 135, 121, 104, 91, 79, 65, 51. FTIR (KBr, cm<sup>-1</sup>): 3089, 2925, 2889, 1525, 1348, 1205, 1097, 1064, 953, 735.  $\epsilon_{313}$  (MeOH) = 1400 dm<sup>3</sup> mol<sup>-1</sup> cm<sup>-1</sup>,  $\epsilon_{366}$  (MeOH) = 280 dm<sup>3</sup> mol<sup>-1</sup> cm<sup>-1</sup>. Anal. Calcd for C<sub>15</sub>H<sub>12</sub>N<sub>2</sub>O<sub>6</sub>: C, 56.96; H, 3.82; N, 8.86. Found: C, 56.94; H, 3.81; N, 8.83.

**2-(2-Nitrophenyl)-1,3-oxathiolane (4).** Prepared from **5** in 95% yield; yellowish crystals. Mp 57.5–60.0 °C. <sup>1</sup>H NMR (300 MHz, CDCl<sub>3</sub>):  $\delta$  (ppm) 3.12 (m, 2H), 4.03 (dd, 1H,  $J_1 = 14.9$  Hz,  $J_2 = 8.8$  Hz,  $J_3 = 1.6$  Hz), 4.58 (m, 1H), 6.57 (s, 1H), 7.44 (t, 1H,  $J = 7.8$  Hz), 7.64 (t, 1H,  $J = 7.4$  Hz), 7.86 (d, 1H,  $J = 7.9$  Hz), 8.01 (d, 1H,  $J = 7.9$  Hz). <sup>13</sup>C NMR (75.5 MHz, CDCl<sub>3</sub>):  $\delta$  (ppm) 33.2; 72.7; 82.1; 124.8; 127.4; 128.8; 134.0; 137.7; 146.8. MS (EI,  $m/z$ ): 210, 194, 166, 151, 136, 121, 104, 93, 77, 60, 51. FTIR (KBr, cm<sup>-1</sup>): 2940, 2894, 1606, 1515, 1349, 1209, 1064, 977, 717, 674. UV-vis:  $\epsilon_{313}$  (MeOH) = 600 dm<sup>3</sup> mol<sup>-1</sup> cm<sup>-1</sup>,  $\epsilon_{366}$  (MeOH) = 200 dm<sup>3</sup> mol<sup>-1</sup> cm<sup>-1</sup>,  $\epsilon_{313}$  (cyclohexane) = 410 dm<sup>3</sup> mol<sup>-1</sup> cm<sup>-1</sup>,  $\epsilon_{366}$  (cyclohexane) = 160 dm<sup>3</sup> mol<sup>-1</sup> cm<sup>-1</sup>. HRMS (EI+) for C<sub>9</sub>H<sub>9</sub>NO<sub>3</sub>S (M<sup>+</sup>) 211.0303, found 211.0338.

**Synthesis of the Methyl- $\alpha$ -D-glucopyranoside 1g.** Methyl- $\alpha$ -D-glucopyranoside (0.70 g; 3.61 mmol) and 2-nitrobenzaldehyde (0.55 g; 3.64 mmol) were dissolved in dry dioxane (20 mL) under argon atmosphere and concentrated sulfuric acid (0.5 mL) was added dropwise within few minutes according to the literature.<sup>36,37</sup> The reaction mixture was vigorously stirred and the reaction progress was monitored by TLC.

When the conversion reached the maximum (or reaction stopped after 16 days), dichloromethane (20 mL) was added, and the mixture was neutralized with solid Na<sub>2</sub>CO<sub>3</sub> (~1 g). The mixture was filtered and the solvents were removed under reduced pressure. The remaining matter was dissolved in dichloromethane (40 mL) and washed with water (20 mL). The organic phase was dried over MgSO<sub>4</sub>, filtered, and the solvent was evaporated under reduced pressure. Crude product was

purified by flash chromatography to give **1g** in 36% yield. Yellow crystals. Mp 168.8–172.3 °C. <sup>1</sup>H NMR (300 MHz, CDCl<sub>3</sub>):  $\delta$  (ppm) 1.72 (b, 2H), 3.46 (s, 3H), 3.54 (t, 1H,  $J = 8.9$  Hz), 3.64 (dd, 1H,  $J_1 = 9.1$  Hz,  $J_2 = 3.8$  Hz), 3.78 (d, 2H,  $J = 7.3$  Hz), 3.92 (t, 1H,  $J = 9.2$  Hz), 4.27 (d, 1H,  $J = 5.3$  Hz), 4.81 (d, 1H,  $J = 4.0$  Hz), 6.15 (s, 1H), 7.51 (dt, 1H,  $J_1 = 7.8$  Hz,  $J_2 = 0.9$  Hz), 7.63 (t, 1H,  $J = 7.1$  Hz), 7.89 (t, 2H,  $J = 7.8$  Hz). <sup>13</sup>C NMR (75.5 MHz, CDCl<sub>3</sub>):  $\delta$  (ppm) 55.9; 62.5; 69.4; 72.0; 73.2; 81.3; 97.6; 100.0; 124.4; 128.1; 130.1; 131.3; 133.0; 148.6. MS (EI,  $m/z$ ): 285, 224, 207, 194, 178, 152, 135, 121, 104, 73, 60. FTIR (KBr, cm<sup>-1</sup>): 3400, 2940, 1535, 1375, 1354, 1340, 1070, 1040, 1024, 1001, 959, 852, 744, 696.  $\epsilon_{313}$  (MeOH) = 650 dm<sup>3</sup> mol<sup>-1</sup> cm<sup>-1</sup>,  $\epsilon_{366}$  (MeOH) = 200 dm<sup>3</sup> mol<sup>-1</sup> cm<sup>-1</sup>. HRMS (EI+) for C<sub>14</sub>H<sub>17</sub>NO<sub>8</sub> (M<sup>+</sup>) 327.0954, found 327.0943.

**Photolysis of Acetals 1a–f.** Two general methods for the release of the dihydroxy compounds **1a–f** were carried out as follows.

**(A) Stepwise Deprotection.** An acetal (1 mmol) was dissolved in benzene (70 mL), purged with argon for 15 min, and irradiated with a 125-W Hg medium-pressure UV lamp through a Pyrex filter. No starting material was observed usually after 60 min (TLC or GC). The solvent was removed under reduced pressure, and the residue was dissolved in methanolic solution of NaOH (250 mg of NaOH in 50 mL). The reaction mixture was stirred for ~1 h at 20 °C. Solvent was then removed under reduced pressure, and the remaining solid was dissolved in ethyl acetate (20 mL) and washed by water/brine mixture (1:1 v/v; 20 mL). The water layer was then washed with ethyl acetate (2 × 20 mL). Combined organic phases were dried (MgSO<sub>4</sub>), and solvent was removed under reduced pressure. A crude dihydroxy compound was obtained and purified by column chromatography. Their identification was based on comparing the NMR, GC, GC-MS data to those of the authentic compounds. The chemical yields are reported in Table 1.

**(B) One-Pot Deprotection.** An acetal (1 mmol) was dissolved in methanolic solution of NaOH (250 mg of NaOH in 50 mL). The solution was purged with argon for 15 min and irradiated with a 125-W Hg medium-pressure UV lamp through a Pyrex filter for several hours (TLC). The solvent was then removed under reduced pressure and the remaining solid was worked up and the products were identified in the same way as described above. The chemical yields are reported in Table 1.

**Irradiation Experiments in NMR Cuvettes.** A solution of an acetal or the monothioacetal **4** (usually 2–10 mg) in deuterated solvent (500  $\mu$ L) in NMR tube was purged by argon for 10 min. In some experiments involving **4**, ascorbic acid (3–5 molar equiv) was added. The samples were irradiated with a 125-W Hg medium-pressure UV lamp through a Pyrex filter (> 280 nm). In some cases, a solution of NaOD in MeOD was added to carry out the hydrolysis step (a stepwise protocol). <sup>1</sup>H NMR and <sup>13</sup>C-APT NMR spectra were measured in the time intervals as necessary (see Supporting Information). Identification of the (photo)products was based on comparing the analytical data to those of the authentic compounds.

**Quantum Yield Measurements.** The quantum yield measurements were performed on an optical bench consisting of high pressure 350-W or 450-W UV lamps, a 1/8 m monochromator with 200–1600 nm grating, set to 313 nm, and a 1.0-cm matched quartz cell containing a solution degassed purging with argon for 10 min. The sample temperature was maintained using a Peltier thermo block set to 20 °C. The light intensity was monitored by a Si photodiode detector (UV enhanced) with a multifunction optical power meter. The concentration of all sample solutions was approximately 5 × 10<sup>-3</sup> M, containing hexadecane (10<sup>-3</sup> M) for GC analyses as internal standard. 2-Nitrobenzaldehyde or valerophenone were used as actinometers (see the footnote in Table 2). The reaction conversions were always kept below 10% to avoid the interference

of photoproducts. The relative standard deviations for multiple (at least five) samples were found below 10% in all analyses.

**Irradiation of 1e in D<sub>2</sub><sup>18</sup>O.** A solution of 1e (10.0 mg) in C<sub>6</sub>D<sub>6</sub> or CD<sub>3</sub>OD (1 mL) was transferred to two NMR tubes; one drop of D<sub>2</sub><sup>16</sup>O was added into the first tube, and one drop of D<sub>2</sub><sup>18</sup>O was added to the second tube. Both samples were purged by argon for 10 min and were irradiated with a 125-W Hg medium-pressure UV lamp through a Pyrex filter (> 280 nm). When the reaction reached a full conversion (NMR), the solutions were analyzed by HPLC-MS.

**Acknowledgment.** The project was supported by the Grant Agency of the Czech Republic (203/09/0748) and by the Czech Ministry of Education, Youth and Sport (MSM0021622413). The authors express their thanks to Thomas Bally, Michal Cajan, Richard S. Givens, Otakar

Humpa, Zdenek Kriz, Petr Kukucka, Romana Kurkova, and Radek Marek for their help with the quantum-chemical calculations and chemical analyses, and for fruitful discussions. The University of Fribourg and CESNET association are acknowledged for the computational resources.

**Supporting Information Available:** Experimental section including materials, methods and quantum-chemical calculations; synthesis and photolysis of 5-*tert*-butyl-2-(2-nitrophenyl)benzo[*d*][1,3]dioxole; <sup>1</sup>H–<sup>1</sup>H COSY and <sup>1</sup>H–<sup>13</sup>C HMBC NMR correlations; the total energies (including scaled ZPVEs) and the total Gibbs energies (with scaled thermal corrections) of calculated neutral and anionic species discussed in the article; calculated optimized structures with the corresponding transition states. This material is available free of charge via the Internet at <http://pubs.acs.org>.